Defects in Peroxisomal 6-Phosphogluconate Dehydrogenase Isoform *PGD2* Prevent Gametophytic Interaction in *Arabidopsis thaliana*[1][OPEN]

Christian Hölscher[2], Marie-Christin Lutterbey[2], Hannes Lansing, Tanja Meyer, Kerstin Fischer, and Antje von Schaewen*

Institut für Biologie und Biotechnologie der Pflanzen, Westfälische Wilhelms-Universität Münster, Schlossplatz 7, D-48149 Münster, Germany

ORCID IDs: 0000-0003-0869-1320 (M.-C.L.); 0000-0001-5716-2877 (H.L.); 0000-0003-0832-108X (A.v.S.).

We studied the localization of 6-phosphogluconate dehydrogenase (PGD) isoforms of Arabidopsis (*Arabidopsis thaliana*). Similar polypeptide lengths of PGD1, PGD2, and PGD3 obscured which isoform may represent the cytosolic and/or plastidic enzyme plus whether PGD2 with a peroxisomal targeting motif also might target plastids. Reporter-fusion analyses in protoplasts revealed that, with a free N terminus, PGD1 and PGD3 accumulate in the cytosol and chloroplasts, whereas PGD2 remains in the cytosol. Mutagenesis of a conserved second ATG enhanced the plastidic localization of PGD1 and PGD3 but not PGD2. Amino-terminal deletions of PGD2 fusions with a free C terminus resulted in peroxisomal import after dimerization, and PGD2 could be immunodetected in purified peroxisomes. Repeated selfing of *pgd2* transfer (T-)DNA alleles yielded no homozygous mutants, although siliques and seeds of heterozygous plants developed normally. Detailed analyses of the C-terminally truncated PGD2-1 protein showed that peroxisomal import and catalytic activity are abolished. Reciprocal backcrosses of *pgd2-1* suggested that missing PGD activity in peroxisomes primarily affects the male gametophyte. Tetrad analyses in the *quartet1-2* background revealed that *pgd2-1* pollen is vital and in vitro germination normal, but pollen tube growth inside stylar tissues appeared less directed. Mutual gametophytic sterility was overcome by complementation with a genomic construct but not with a version lacking the first ATG. These analyses showed that peroxisomal PGD2 activity is required for guided growth of the male gametophytes and pollen tube-ovule interaction. Our report finally demonstrates an essential role of oxidative pentose-phosphate pathway reactions in peroxisomes, likely needed to sustain critical levels of nitric oxide and/or jasmonic acid, whose biosynthesis both depend on NADPH provision.

The oxidative pentose-phosphate pathway (OPPP) is an important metabolic route to retrieve reduction power from soluble sugars (Kruger and von Schaewen, 2003). The sequential action of three enzymes, namely glucose-6-phosphate dehydrogenase (G6PDH), 6-phosphogluconolactonase (6PGL), and 6-phosphogluconate dehydrogenase (6PGDH), results in the conversion of Glc-6-P to ribulose-5-phosphate (Ru-5-P), yielding NADPH at the expense of CO_2. Ru-5-P is an important precursor of nucleotide biosynthesis, both in the cytosol and inside plastids. The 2 mol of NADPH produced by the dehydrogenase reactions support reductive biosynthesis (e.g. nucleotides, amino acids, or fatty acids) and contribute to glutathione-based redox homeostasis (GSH/GSSG ratio) in various cellular compartments. Mainly, this occurs through the NADPH-dependent glutathione reductase step, which is central to the ascorbate-glutathione pathway during the recovery from oxidative stress (for review, see Noctor et al., 2012).

In plant cells, the complete OPPP operates in plastids (Schnarrenberger et al., 1995) and in chloroplasts at night as a formal reversion of the Calvin-Benson cycle (Buchanan, 1991; Scheibe, 1991; Kruger and von Schaewen, 2003). The three irreversible OPPP reactions also are present in the cytosol but probably only transiently in peroxisomes (Meyer et al., 2011; Hölscher et al., 2014). The latter had been first suggested upon immunodetection of G6PDH in purified pea (*Pisum sativum*) peroxisomes (Corpas et al., 1998). Besides, the OPPP may play a role during lipid mobilization (Graham and Eastmond, 2002), because NADPH is required for the degradation of odd-unsaturated fatty acids (via 2*E*,4*E*-dienoyl-CoA reductase) that occurs mainly in peroxisomes of higher plants (Goepfert and

[1] This work was supported by the Deutsche Forschungsgemeinschaft (grant no. DFG SCHA 541/12–1 to A.v.S.).

[2] These authors contributed equally to the article.

* Address correspondence to schaewen@uni-muenster.de.

The author responsible for distribution of materials integral to the findings presented in this article in accordance with the policy described in the Instructions for Authors (www.plantphysiol.org) is: Antje von Schaewen (schaewen@uni-muenster.de).

C.H., M.-C.L., H.L., T.M., and K.F. designed/performed experiments and analyzed data; A.v.S. designed experiments and analyzed data; A.v.S. and C.H. wrote the article; all authors read and approved the final version of the article.

[OPEN] Articles can be viewed without a subscription.

www.plantphysiol.org/cgi/doi/10.1104/pp.15.01301

Poirier, 2007). Recently, NADPH production in peroxisomes was shown to be important for the biosynthesis of nitric oxide (NO) in roots facing abiotic stress, either induced by salt (NaCl; Corpas et al., 2009) or heavy metals (cadmium; Corpas and Barroso, 2014a). Whether peroxisomal NADPH may be needed for NO synthesis, which plays an important role during fertilization (Prado et al., 2004, 2008), remained unclear, mainly because, aside from the OPPP, NADPH in peroxisomes also can be produced by other enzymes, such as NADP-dependent isocitrate dehydrogenase (NADP-ICDH; At1g54340) with peroxisomal targeting signal type 1 (PTS1) motif SRL (Reumann et al., 2004; Leterrier et al., 2012) or stress-related phosphorylation of NAD(H) via the NAD kinase isoform NADK3 (Chai et al., 2006) with PTS1 motif SRY (Waller et al., 2010). Hence, under which conditions OPPP reactions in peroxisomes may be necessary or even essential remained to be determined.

We previously analyzed the subcellular targeting of Arabidopsis (*Arabidopsis thaliana*) OPPP enzymes, first of the six *G6PD* isoforms (Meyer et al., 2011) and then of the five *6PGL* isoforms (Hölscher et al., 2014). Based on these results, we came up with a model for how the first two OPPP steps may be redirected from chloroplasts to peroxisomes upon redox change(s) in the cytosol: stress or developmental cues trigger the interaction of G6PD4 with the plastid-destined G6PD1 precursor in the cytosol after initiation by a cognate thioredoxin (Trx *m2*). In mesophyll cells, Trx *m2* coexpression resulted in the folding of G6PD1 in the cytosol and uptake into peroxisomes via the exposition of an internal PTS1-like motif within the C terminus (Meyer et al., 2011). For the second OPPP step, dual targeting of PGL3 to plastids and/or peroxisomes was found to be influenced by Trx *m2* as well, here acting as a redox-sensitive cochaperone promoting Trx *holdase* activity in the reduced state but *foldase* activity in the oxidized state (Hölscher et al., 2014).

The possible importance of OPPP reactions inside plastids and/or peroxisomes for reproductive development is indicated by embryo- or pollen-defective genes in Arabidopsis. Transfer DNA (T-DNA) insertions either abolishing the activity of PGL3 (At5g24400, listed as emb2024; Meinke et al., 2008) or PGD2 (At3g02360, described as pollen defective in Niewiadomski et al., 2005) are apparently homozygous lethal. PGL3, which can dually target plastids and peroxisomes (Hölscher et al., 2014), was found to be mostly required in plastids (Xiong et al., 2009; Bussell et al., 2013), whereas PGD2 was identified in the peroxisomal proteome of both dark-adapted Arabidopsis leaves (Reumann et al., 2007) and etiolated tissues (Eubel et al., 2008; Quan et al., 2013). However, whether PGD2 may dually target plastids and peroxisomes (like OPPP isoforms G6PD1 and PGL3) remained unclear.

To settle these issues, the subcellular localization of all Arabidopsis *PGD* family members was studied in tobacco (*Nicotiana tabacum*) and Arabidopsis protoplasts. This revealed that PGD2 is only imported by peroxisomes but not by chloroplasts. Nevertheless, no homozygous *pgd2-1* or *pgd2-2* mutants were found among the progeny of heterozygous plants. Detailed analyses of the C-terminally altered PGD2-1 protein, plus complementation analysis of the corresponding *pgd2-1* mutant by genomic constructs, revealed an important role for peroxisomal OPPP reactions during fertilization.

RESULTS

N-Terminal Targeting Analyses of the Three Arabidopsis PGD Isoforms

Based on phylogenetic analyses, Arabidopsis PGD1 (At1g64190) and PGD3 (At5g41670) were classified as plastidic orthologs, and PGD2 (At3g02360) was classified as a cytosolic ortholog, of the corresponding spinach (*Spinacia oleracea*) 6PGDH enzymes (Krepinsky et al., 2001). However, by contrast to spinach, none of the Arabidopsis PGD isoforms exhibits an N-terminal extension indicative of a plastidic transit peptide (Fig. 1A; Supplemental Fig. S1A). Notably, upon BLASTp search with PGD2, no other Arabidopsis PGD isoforms were retrieved, and PTS1 motifs are conserved among the listed higher plant homologs (Supplemental Fig. S1B). Transient expression of the three PGD-reporter fusions with the free N-terminal end in sugar-adapted tobacco protoplasts showed that monomeric red fluorescent protein (mRFP)-based PGD1- and PGD3-OFP fusions accumulate in both the cytosol and chloroplasts (Fig. 1B, a, b, d, and e) as well as with the 5′ untranslated region (UTR; data not shown). Localization in the stroma was confirmed by coexpression with a reporter construct in which yellow fluorescent protein (YFP) is fused to the transit peptide of ferredoxin-NADP reductase (FNR_*tp*-YFP; Fig. 1B, b and e, white signals). Mutagenesis of the second ATG, which is conserved in all *PGD* isoforms (Fig. 1A, red frame), resulted in enhanced but not exclusive labeling of the chloroplast stroma (Fig. 1B, c and f; for separate channels, see Supplemental Fig. S2), indicating that dual localization (cytosol/plastids) of PGD1 and PGD3 may be regulated not by an alternative translation but by a different mechanism. In contrast, PGD2 remained in the cytosol (Fig. 1B, g), even when including the 5′ UTR (Fig. 1B, h) or with a mutagenized second ATG (Fig. 1B, i). Importantly, unlike the previous findings for G6PD1 (Meyer et al., 2011) and PGL3 (Hölscher et al., 2014), coexpression of Trx *m2*-reporter fusions did not influence the localization of the PGD2_*N-full* version (data not shown).

C-Terminal Targeting Analyses of PGD2

PGD2 was identified previously in the proteome of peroxisomes isolated from dark-adapted Arabidopsis leaves (Reumann et al., 2007). Yet, a full-length EYFP-PGD2 fusion remained in the cytosol of

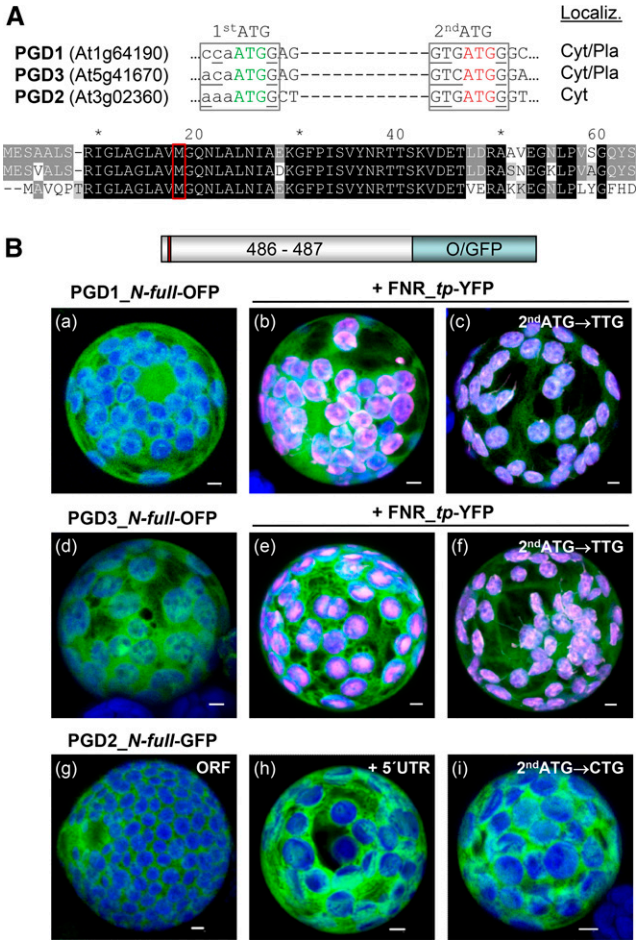

Figure 1. Localization of full-length PGD1-, PGD3-, and PGD2-reporter fusions. A, Details of the DNA sequence (top) and alignment of the N-terminal ends of the three Arabidopsis PGD isoforms (bottom). A potential second start codon (2ndATG) with Kozak consensus (bases underlined) in all isoforms is highlighted in red. Cyt/Pla, Cytosol/plastids. B, Transient expression of the indicated fusion constructs in tobacco protoplasts (48 h post transfection). PGD3 (a) and PGD1 (d) accumulate in both cytosol and chloroplasts, as confirmed by colocalization with a transit peptide fusion of ferredoxin-NADP reductase (FNR_*tp*-YFP; b and e). Silent mutagenesis of the second ATG in PGD1 and PGD3 results in enhanced labeling of chloroplasts (c and f). PGD2 labels the cytosol (g) as well as with the 5′ UTR (h) or mutated second ATG (i). Only maximal projections (of approximately 35 single sections) are shown (for single-channel images, see Supplemental Figs. S2 and S4). Candidate fusions are in green, chloroplast marker (FNR) is in magenta, and chlorophyll autofluorescence is in blue. Colocalization and very close signals (less than 200 nm) appear white in merged images. ORF, Open reading frame. Bars = 3 μm.

particle-bombarded onion (*Allium cepa*) epidermal cells (Reumann et al., 2007). Therefore, we cloned various truncated fusions, plus a full-length cyan fluorescent protein (CFP)-PGD2 version, to test the effect of N-terminal deletions, beginning with the second Met down to 75 residual amino acids with an intact C-terminal PTS1 motif SKI (Fig. 2A). As indicated by coexpression with the peroxisomal marker PGL3_*C-short* (Meyer et al., 2011), all N-terminally truncated PGD2 versions are imported by peroxisomes (Fig. 2B, a–c). However, with a mutated PTS1 motif (Fig. 2A, PGD2_*C-mature*-SEI) or as a C-terminal full-length fusion, PGD2 remained in the cytosol (Fig. 2B, d and e). The latter confirms the result obtained with EYFP-PGD2 in onion (Reumann et al., 2007). Yet, a single amino acid change in the minor PTS1 motif SKI toward the major PTS1 motif SKL (Reumann, 2004) also resulted in peroxisomal import of the full-length CFP-PGD2 version (Fig. 2B, f; for single-channel images, see Supplemental Fig. S4).

BiFC Analyses Show That PGD2 Dimerizes in the Cytosol Prior to Peroxisome Import

Based on the three-dimensional structure of the homolog from *Trypanosoma brucei*, 6PGDH enzymes are

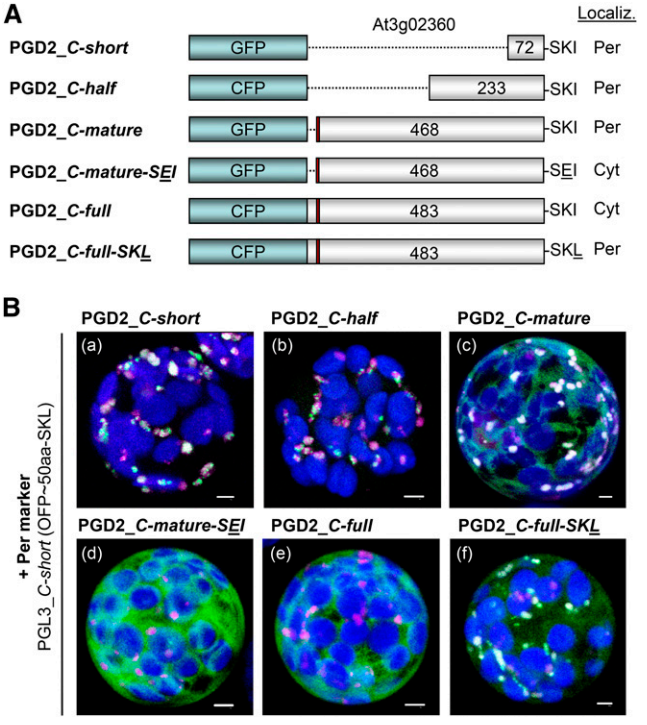

Figure 2. Analysis of reporter-PGD2 fusions. A, Schemes of the reporter-PGD2 fusions with intact or modified C-terminal ends (the position of the second ATG is marked in red) and their localization. Cyt, Cytosol; Per, peroxisomes. B, Transient expression of the indicated fusions in tobacco protoplasts (48 h post transfection). Only merged images of all channels are shown. All truncated PGD2 fusions with free C terminus localize to peroxisomes (a–c), unless PTS1 motif SKI is mutated to SEI, here shown for the mature version (d). The full-length CFP-PGD2 version remains in the cytosol (e) as EYFP-PGD2 (Reumann et al., 2007), unless PTS1 motif SKI is changed to SKL (f). Only maximal projections (of approximately 35 single sections) are shown (for single-channel images, see Supplemental Fig. S3). Candidate fusions are in green the peroxisome marker PGL3_*C-short* (Meyer et al., 2011) is in magenta, and chlorophyll autofluorescence is in blue. Colocalization and very close signals (less than 200 nm) appear white in merged images. Bars = 3 μm.

dimers with intertwined C termini that form part of the catalytic site (Phillips et al., 1998). To investigate whether PGD2 dimerizes in the cytosol or within peroxisomes, we cloned split YFP-reporter fusions to study full-length versus mature PGD2 versions by in planta BiFC (Walter et al., 2004). Coexpression in tobacco mesophyll protoplasts revealed that all four full-length PGD2 combinations interact in the cytosol, independent of whether the reporter masks the C-terminal end or not (Fig. 3, a, c, e, and g). By contrast, only the mature PGD2 combination in which both C-terminal ends are freely accessible accumulated in peroxisomes (Fig. 3, h). This also was the case in Arabidopsis protoplasts, both of soil-grown and sugar-adapted plants, which gave similar results (Supplemental Figs. S4 and S5). Thus, our BiFC results confirmed the data obtained with undivided reporters fused to mature or full-length PGD2 (Fig. 2B, c and e). Moreover, detection of both cytosolic and peroxisomal signals within single cells revealed that PGD2 dimerizes in the cytosol prior to import into peroxisomes. This is in agreement with the fact that peroxisomes only import completely folded and assembled proteins, or even larger protein complexes, across their membranes (Hu et al., 2012). Together, these analyses indicate that *PGD2* encodes a peroxisomal 6PGDH that is unable to enter plastids.

Immunodetection of PGD2 in Purified Peroxisomes

To analyze whether PGD2 protein copurifies with peroxisomes, we isolated the peroxisomal fraction of Arabidopsis wild-type leaves. Glycolate oxidase was used as a peroxisome tracker and non-phosphorylating glyceraldehyde-3-phosphate dehydrogenase (GAPN) as a cytosolic reference. While 6PGDH and G6PDH activity could be detected in the purified peroxisome fraction (Fig. 4A, Per), no GAPN activity was found. This indicated little to no cytosolic contamination. PGD proteins were analyzed by western blotting using a newly generated His-PGD2 antiserum (recognizing all recombinant PGD isoforms; data not shown). Aliquots of the crude extract and purified peroxisomes with similar 6PGDH activity gave rise to comparable α-PGD signals (Fig. 4B, asterisk). Since the stroma marker Rubisco large subunit was absent from the peroxisomal fraction (Fig. 4B, arrowhead), PGD1 and PGD3 isoforms likely do not contribute significantly. Thus, PGD2 is indeed present in peroxisomes.

Lack of Homozygous *pgd2* Plants Is Linked to Missing 6PGDH Activity in Peroxisomes

To substantiate a role for OPPP reactions in peroxisomes based on T-DNA insertion lines, we investigated two mutant alleles of *PGD2* (At3g02360): SALK_036751, termed *pgd2-1*, and SALK_071687, termed *pgd2-2* (Fig. 5A). No homozygous plants were found for either line (Table I), although in *pgd2-1*, the T-DNA is inserted at the very end of the coding region, resulting in replacement of the last 24 amino acids with 17 unrelated amino acids. As shown in Figure 5B, this change prevented peroxisomal import of a GFP-based PGD2-1_*C-mature* version. Moreover, the C-terminal alteration abolished 6PGDH activity (Fig. 5C), as determined by measurement of purified recombinant PGD2 and PGD2-1 proteins with an N-terminal His-tag (Supplemental Fig. S6). Thus, even the slightly altered *pgd2-1* allele is unlikely to be leaky.

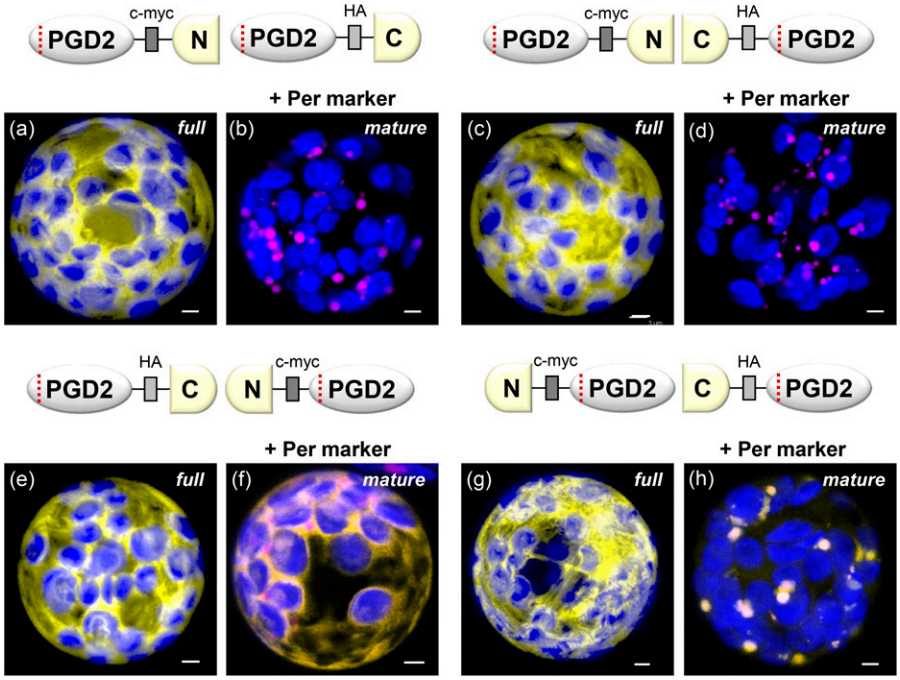

Figure 3. BiFC analysis of *full-length* versus *mature* PGD2 split YFP combinations in tobacco protoplasts (48 h post transfection). Independent of N- or C-terminal fusion, all full-length PGD2 versions dimerize in the cytosol (panels a,c,e,g), but are not imported by peroxisomes, even when both C-terminal ends are free (panel g). In case of the mature PGD2 versions, only the combination with two free C-terminal ends is imported by peroxisomes after dimerization in the cytosol (panel h; also in Arabidopsis protoplasts, Fig. S5), but not when only one C-terminal end is free (panel f). For two of the mature PGD2 combinations no reconstituted YFP signals were found (panels b and d). Only maximal projections (of ~35 single sections) are shown. Candidate fusions in yellow, peroxisome marker (PGL3_*C-short*) in magenta, and chlorophyll autofluorescence in blue. Co-localization and very close signals (< 200 nm) appear white in merged images of all channels. Scale bars = 3 μm.

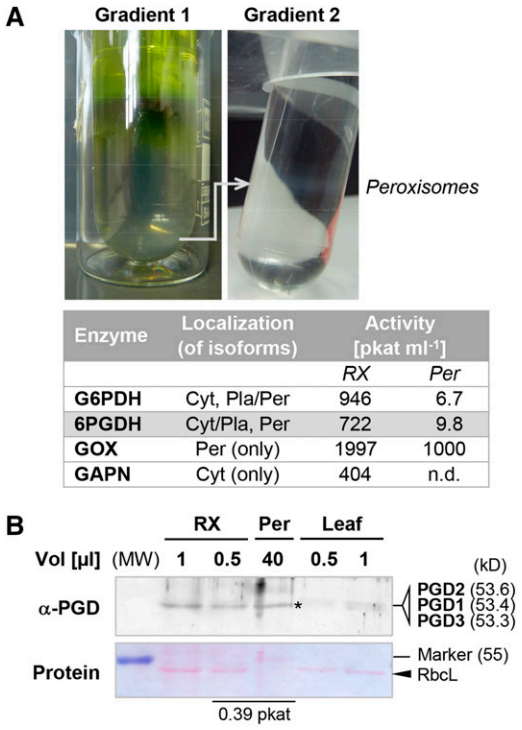

Enzyme	Localization (of isoforms)	Activity [pkat ml^{-1}]	
		RX	*Per*
G6PDH	Cyt, Pla/Per	946	6.7
6PGDH	Cyt/Pla, Per	722	9.8
GOX	Per (only)	1997	1000
GAPN	Cyt (only)	404	n.d.

Figure 4. Purification of Arabidopsis leaf peroxisomes and immunodetection of PGD2. A, Top, Percoll/Suc (1) and Suc (2) gradients after centrifugation of 34 mL of crude extract, resulting in a band of purified peroxisomes (0.9 mL). Bottom, Table of G6PDH and 6PGDH activity, with glycolate oxidase (GOX) serving as the peroxisomal reference and nonphosphorylating GAPN as the cytosolic reference. In Arabidopsis, several isoenzymes may contribute to G6PDH (five isoforms) and 6PGDH (three isoforms) activity. Cyt, Cytosol; n.d., not detected; Pla, plastids; Per, peroxisomes; RX, crude extract. B, Immunoblot developed with the new His-PGD2 antiserum (α-PGD). Aliquots of crude extract, purified peroxisomes, and a thawed leaf extract were loaded next to each other. Crude extract and peroxisomes of similar 6PGDH activity (0.39 pkat) give comparable signals (asterisk). Together with the lack of GAPN activity (A, table), the missing band of Rubisco large subunit (RbcL) from the peroxisome fraction indicates little contribution of dually cytosolic/plastidial PGD1 and PGD3 isoforms of similar size (kD; in parentheses). MW, Molecular weight standard (PageRuler; Fermentas).

Analysis of *pgd2-1* in the *quartet1-2* Background Reveals Mutual Gametophytic Sterility

Repeated selfing of heterozygous plants did not yield homozygous individuals for either of the two *pgd2* alleles (Table I), in line with previously proposed male gametophytic defects (Niewiadomski et al., 2005). To enable more detailed studies, we introgressed a *quartet* (*qrt*) mutant (Preuss et al., 1994) by pollinating heterozygous *PGD2 pgd2-1* stigmas with *qrt1-2* (Supplemental Fig. S7), which is defective in a pectin methylesterase (Francis et al., 2006). Genotypic distribution in the F1 generation was about normal (Table II; 54% heterozygous progeny), excluding solely female gametophytic defects. Significant deviations from Mendelian genetics were again found in the F2 generation (Table II). In *qrt* mutants, analysis of the male gametophytes is facilitated by the nonseparation of pollen tetrads (Preuss et al., 1994). All pollen grains of *PGD2 pgd2-1* tetrads were vital and germinated on Suc-containing medium (Fig. 6A). These results excluded the possibility of toxic effects of missing 6PGDH activity in the haploid state, which was confirmed by reciprocal backcrosses. Zero transmission through mutant pollen would indicate male sterility of the *pgd2* alleles, but for wild-type pistils pollinated by *PGD2 pgd2-1* and vice versa, only a slight reduction in heterozygous offspring was recorded (Table I; approximately 40% instead of the expected 50%). These analyses showed that *pgd2-1* ovules can be fertilized by wild-type pollen tubes, and vice versa, *pgd2-1* pollen tubes successfully compete for the fertilization of wild-type ovules. The latter is consistent with Suc (imported from stylar tissues; Leydon et al., 2014) being the primary energy source for pollen tube growth, mainly involving OPPP reactions in plastids (Selinski and Scheibe, 2014). However, *pgd2-1* pollen tubes with

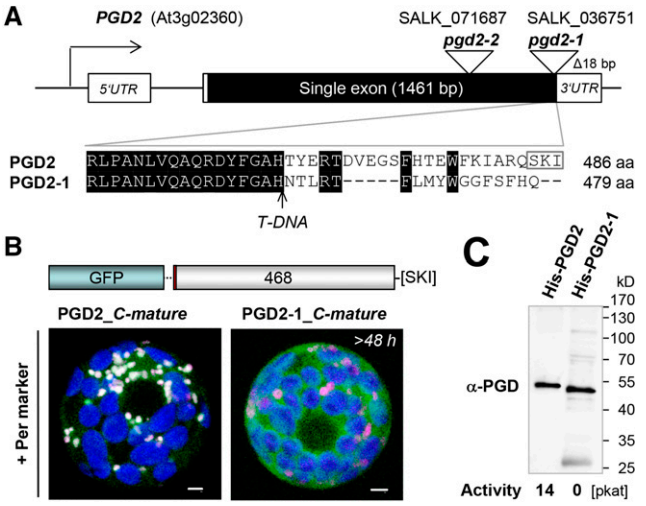

Figure 5. Subcellular localization and activity of PGD2 and C-terminally altered PGD2-1. A, Top, Scheme of the At3g02360 locus and positions of T-DNA insertions (triangles) in the single exon of *PGD2*. Bottom, C-terminal amino acid alignment of PGD2 and PGD2-1. The position of the T-DNA insertion is marked by the arrow, and the PTS1 motif is indicated by the gray frame. aa, Amino acids. B, Transient expression of mature PGD2 and PGD2-1 fusions in tobacco protoplasts (more than 48 h post transfection). By contrast to PGD2, PGD2-1 (with an altered C terminus) accumulates in the cytosol. Only maximal projections (of approximately 35 single sections) are shown. Candidate fusions are in green, the peroxisome (Per) marker PGL3_*C-short* (Meyer et al., 2011) is in magenta, and chlorophyll autofluorescence is in blue. Colocalization and very close signals (less than 200 nm) appear white in merged images. Bars = 3 µm. C, Activity test of purified His-PGD2 and His-PGD2-1 variants expressed in the *G6PD*-deficient *E. coli* strain BL21^{minus} (Meyer et al., 2011) upon metal-chelate purification (nickel-nitrilotriacetic acid agarose [Ni-NTA] column). The immunoblot was developed with the His-PGD2 antiserum (α-PGD). 6PGDH activity (in pkat) of the elution fractions with comparable blot signal (Supplemental Fig. S6) is indicated below the blot, and apparent molecular masses (in kD) are given at right.

Table I. *Frequency of wild-type, heterozygous, and homozygous alleles found for the given Arabidopsis T-DNA insertion mutants of peroxisomal isoform PGD2*

Col-0, Columbia-0; wt, wild-type alleles.

PGD2 (At3g02360)	Allele	No.	*PGD2 PGD2*	*PGD2 pgd2*	*pgd2 pgd2*
SALK_071687					
♀ *PGD2 pgd2-2* × ♂ *PGD2 pgd2-2* (selfed)	*pgd2-2* (exon)	50	48%	52%[a]	0%
SALK_036751					
♀ *PGD2 pgd2-1* × ♂ *PGD2 pgd2-1* (selfed)	*pgd2-1* (no PTS1)	278	55%	45%[a]	0%
♀ *PGD2 pgd2-1* × ♂ *PGD2 PGD2* (Col-0 wt)	F1 (reciprocal backcross)	28	60.7%	39.3%[b]	–
♀ *PGD2 PGD2* (Col-0 wt) × ♂ *PGD2 pgd2-1*		43	60.5%	39.5%	–
SALK_036751::*gPGD2* (complementation)	T2[c]	68	29.4%	44.1%	26.5%
SALK_036751::*gPGD2* Δ 1st ATG (complementation)	T2	155	49%	51%	0%

[a]Mean of heterozygous plants after selfing (both *pgd2* alleles and *pgd2-1* in *qrt2-1*; Table II) = 48.6%. [b]Mean of heterozygous plants after female backcrosses (including *qrt2-1*; Table II) = 46.7%. [c]No homozygous T-DNA alleles among T1 plants (n = 114) selected on hygromycin B (Desfeux et al., 2000).

defective peroxisomal OPPP failed to fertilize *pgd2-1* ovules. This was supported by Aniline Blue staining of pollen tubes growing in maternal tissues upon selfing. Pollen tube growth in styles of the wild type (Col-0) and the *qrt1-2* mutant appeared directed compared with the more erratic, undirected growth observed in styles of plants harboring the *pgd2-1* allele (Fig. 6B, compare Col-0 with *PGD2 pgd2-1* and *qrt1-2* with *PGD2 pgd2-1 qrt1-2*).

In developing siliques of heterozygous *PGD2 pgd2-1* plants, most ovaries filled with mature seeds (Fig. 7A) that germinated similarly well to those of the wild type or the *qrt1-2* mutant (Fig. 7B; approximately 10% abortion rate). Thus, from genotypic distribution upon selfing and backcrossing, plus pollen tetrad analyses in the *qrt1-2* mutant background, we conclude that blocking OPPP reactions in peroxisomes leads to mutual gametophytic sterility. This metabolic defect likely affects pollen tube-ovule targeting and/or pollen tube reception by the synergid cells, which ultimately prevents sperm cell delivery to the egg cell (Traverso et al., 2013; see schemes in Leydon et al., 2014) and, thus, the formation of homozygous mutant offspring.

Fertility Is Restored by a Genomic *gPGD2* Construct But Not with a Mutated First ATG

To prove that the mutual sterility of the *pgd2-1* allele is solely caused by a lack of PGD2 activity in peroxisomes, we cloned a genomic *PGD2* fragment (*gPGD2*) comprising 5′ and 3′ regions (Fig. 8A) and created a version with an eliminated first ATG. Surprisingly, the latter showed no catalytic activity as purified His-tagged protein (Supplemental Fig. S8). After transfer to a binary vector and transformation of agrobacteria, heterozygous SALK_036751 plants were subjected to floral dip transformation (Clough and Bent, 1998). *PGD2* and *pgd2-1* loci were scored by genomic PCR in the T1 and T2 generations (Fig. 8B). Homozygous T-DNA alleles were not detected among a total of 114 hygromycin-resistant SALK_036751::*gPGD2* plants. Only after selfing of heterozygous T1 plants were they found in about Mendelian distribution among the T2 progeny of *gPGD2* wild type but not of *gPGD2* $\Delta 1^{st}$ ATG, enforcing the use of the second ATG (Table I; Fig. 8B). These findings strongly indicate that mutual gametophytic sterility is solely caused by the *pgd2-1* allele.

DISCUSSION

Detailed analyses of the three Arabidopsis *PGD* isoforms of about similar size revealed dual targeting for PGD1 and PGD3 to the cytosol and plastid stroma. Due to missing catalytic activity of PGD2 $\Delta 1^{st}$ ATG, this is probably not governed by alternative start codon selection but likely by another mechanism. Regulation of subcellular targeting at the posttranslational level is beneficial for fast local adjustments (e.g. to fluctuating light conditions that can differ dramatically for chloroplasts that are spatially separated within the same

Table II. *Frequency of wild-type, heterozygous, and homozygous alleles found for the Arabidopsis T-DNA allele pgd2-1 in the qrt1-2 background*

CS8846, point mutation in *QRT1* (Preuss et al., 1994; Copenhaver et al., 1998) encoding a pectin methylesterase (Francis et al., 2006).

SALK_036751 × CS8846	(Back)cross	No.	*PGD2 PGD2*	*PGD2 pgd2-1*	*pgd2-1 pgd2-1*
♀ *PGD2 pgd2-1* × ♂ *PGD2 PGD2* (*qrt1-2*)	F1	63	46%	54%[a]	–
♀ *PGD2 pgd2-1*$^{(qrt1-2)}$ × ♂ *PGD2 pgd2-1*$^{(qrt1-2)}$	F2	100	51%	49%[b]	0%

[a]Mean of heterozygous plants after selfing (both *pgd2* alleles and *pgd2-1* in *qrt2-1*; Table I) = 48.6%. [b]Mean of heterozygous plants after female backcrosses (including *qrt2-1*; Table I) = 46.7%.

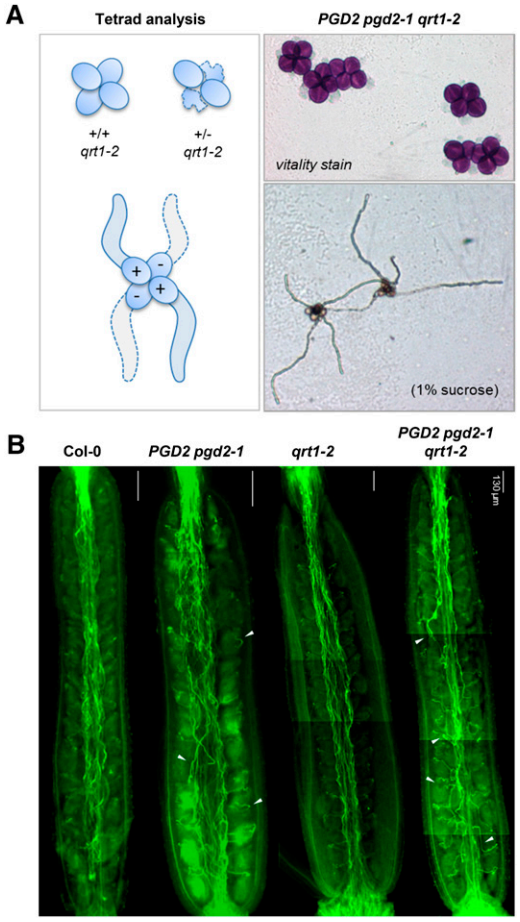

Figure 6. Analysis of *pgd2-1* pollen tube growth in the *qrt1-2* mutant. A, Tetrad analyses of *PGD2 pgd2-1* in the *qrt1-2* background (for details, see Supplemental Fig. S7). Alexander staining (top right) indicates the vitality of all pollen grains. Most *PGD2 pgd2-1* tetrads grew four pollen tubes (like *qrt1-2* alone; data not shown). B, Pollen tube growth in styles of the indicated genotypes visualized by Aniline Blue staining. Note that, compared with Col-0 (wild type) and *qrt1-2*, more pollen tubes of heterozygous *PGD2 pgd2-1* plants grow detours (white arrowheads).

cell; Dietz, 2015). PGD2 of similar size localized to the cytosol (also with its 5′ untranslated leader) and dimerized prior to peroxisomal import. Moreover, we immunodetected PGD2 in purified Arabidopsis leaf peroxisomes. The absence of GAPN and Rubisco large subunit excluded any significant contribution of PGD1 or PGD3. These findings are important for distinguishing between peroxisomal and plastidial defects when studying OPPP isoforms that dually target plastids and peroxisomes. Mutations abrogating OPPP activity in plastids are usually embryo lethal, as exemplified by PGL3 (emb2024; Meinke et al., 2008), the only plastidial PGL isoform of Arabidopsis that alternatively targets peroxisomes (Reumann et al., 2004; Hölscher et al., 2014). Thus, in analogy to *pgl3* mutant alleles abolishing 6PGL activity in plastids (Xiong et al., 2009; Bussell et al., 2013), double mutants of *pgd1* and *pgd3* (lacking plastidial 6PGDH activity) probably also would be lethal.

For unbiased analyses of reduced or missing OPPP activity in peroxisomes, we had to focus on a solely peroxisomal OPPP isoform. *PGD2* was detected previously in the proteome of isolated Arabidopsis peroxisomes (Reumann et al., 2007; Eubel et al., 2008; Quan et al., 2013) but was not imported as an EYFP fusion. Now, we confirm that PGD2 is a veritable *peroxisomal* enzyme and that reporter-PGD2 fusions target peroxisomes but cannot enter plastids. Moreover, a mutant protein with an altered C terminus (PGD2-1) was not imported by peroxisomes and, due to forming part of the catalytic site in 6PGDH enzymes (Phillips et al., 1998), did not retain enzymatic activity. By contrast to an earlier report (Niewiadomski et al., 2005), we could show by

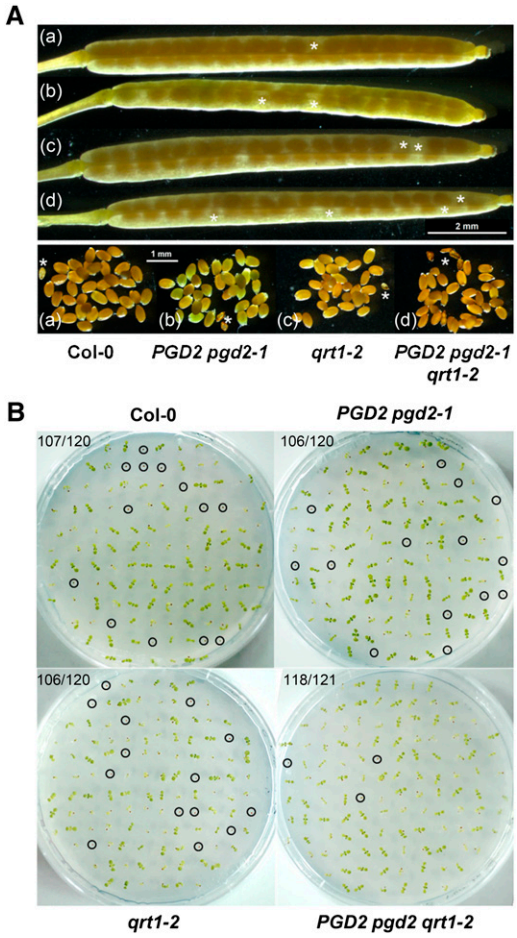

Figure 7. Seed set and germination frequency of *PGD2 pgd2-1* plants. A, Mature siliques with seeds (top) produced by Col-0 wild-type (a), *PGD2 pgd2-1* (b), *qrt1-2* (c), and *PGD2 pgd2-1 qrt1-2* (d) plants; aborted ovules are marked by white asterisks. B, Seed germination test of the indicated genotypes on Murashige and Skoog (MS) agar without Suc (day 15). Nongerminated seeds are marked by circles. A similar germination frequency indicates the absence of female defects; numbers in top left corners refer to germinated seeds versus total seeds analyzed.

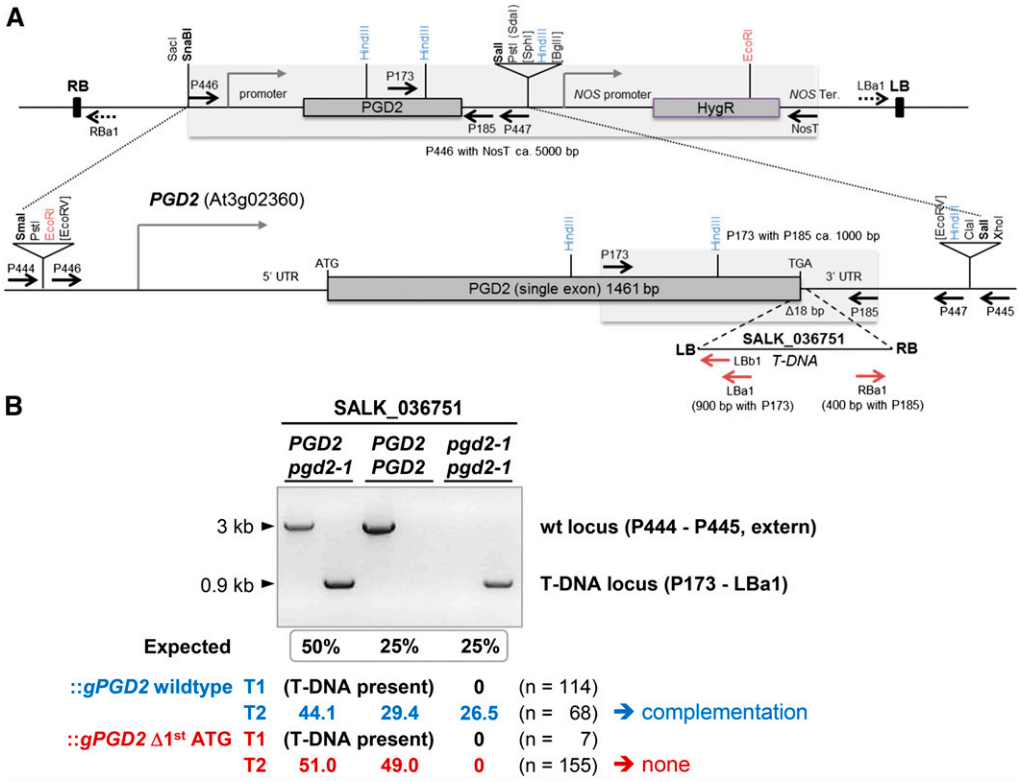

Figure 8. Complementation analysis of *PGD2 pgd2-1* plants after dip transformation with genomic *gPGD2* constructs. A, Top, Scheme of the genomic constructs in binary vector pGSC1704 (with the NOS hygromycin B resistance cassette [HygR]). Bottom, *PGD2* locus (At3g02360) with the position of the T-DNA insert (triangle) in SALK_036751 (termed *pgd2-1*) and the region amplified from wild-type DNA using PCR primers P446 and P447 (dashed lines) to obtain a genomic fragment for mutant complementation. Upon insertion into pBluescript SK, the genomic *gPGD2* fragment with its own promoter and terminator sequences also was mutated using primers with an indicative *Xba*I site (Supplemental Table S1; $\Delta 1^{st}$ ATG [*Xba*I]). Both versions were cloned via SmaI/SalI into *Sna*BI/*Sal*I sites (boldface) in the binary vector. Relevant restriction sites, promoter regions (bent closed arrows), primer-binding sites (arrows; for the T-DNA in red), as well as right (RB) and left (LB) T-DNA borders are indicated. ATG-TGA, Start-stop codons; T/Ter, terminator. B, PCR pattern obtained for the different genotypes (*PGD2* and *pgd2-1*) upon amplification from SALK_036751 transformants harboring either wild-type (wt) *gPGD2* (blue) or the version with the deleted first ATG codon (red), enforcing use of the second ATG (Fig. 1A; Supplemental Fig. S1). For primer-binding sites, see A. Fragment sizes are indicated on the left, and allele ratios (percentage) of hygromycin-resistant T1 and T2 plants are shown below (n = total number of plants analyzed). For the *gPGD2* wild type, seven independent T1 lines were pooled, and for *gPGD2* $\Delta 1^{st}$ ATG, three independent T1 lines were pooled.

backcrossing and tetrad analyses that male *pgd2-1* gametophytes are vital. Yet, complementation of heterozygous plants was detected only in the T2 generation, clearly depending on PGD2 activity. In accordance with a bias for preferential transfection of female tissues (Desfeux et al., 2000), this indicates that floral dip transformation occurred at a point in reproductive development too late to render ovules competent for interaction with *pgd2*-defective pollen tubes. Thus, steps requiring NADPH provision in peroxisomes are likely the key to understanding what might compromise the interaction of male and female *pgd2* gametophytes in heterozygous plants.

Notably, all Arabidopsis mutants in which the biosynthesis of jasmonic acid (JA) is blocked are male sterile and show significantly reduced pollen germination compared with the wild type (Stintzi and Browse, 2000). An Arabidopsis triple mutant (*fad3-2 fad7-2 fad8-1*) that cannot produce JA due to defects in releasing hexadecatrienoic acid (16:3) and linolenic acid (18:3), both precursors of the oxylipin 12-oxophytodienoic acid (OPDA), is sterile (McConn and Browse, 1996). Mutant plants may be rescued by exogenous supply of linolenic acid, OPDA, or JA, but only at stage 12 late in anthesis (Stintzi and Browse, 2000), just before the flower opens. Interestingly, at this stage, also *PGL3* and *PGD2* (Supplemental Fig. S9) are highly expressed (Schmid et al., 2005). The biosynthesis of JA starts in plastids but is completed in peroxisomes (Katsir et al., 2008), where NADPH is consumed in the OPDA reductase (OPR) reaction catalyzed by OPR3 (At2g06050; with PTS1 signal SRL). OPR3 cannot be replaced by any other OPR isoform (Schaller and Stintzi, 2009), and its substrate OPDA has to be imported from plastids (Fig.

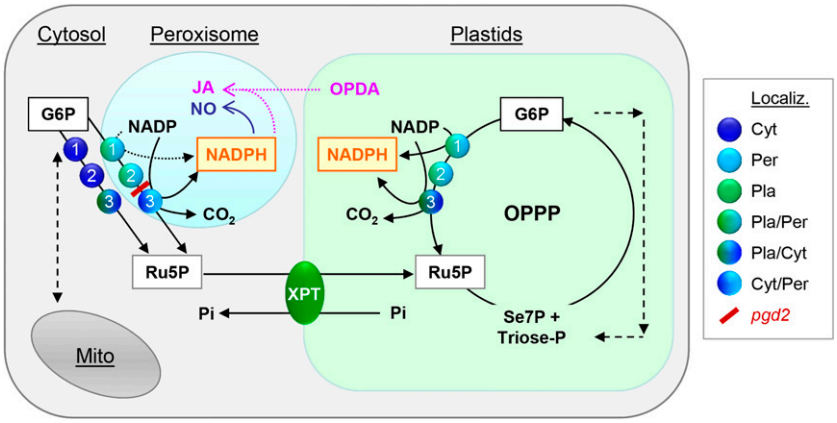

Figure 9. The OPPP as NADPH source in plastids and peroxisomes. The scheme depicts possible compartmentation of OPPP reactions in Arabidopsis. Glucose 6-phosphate dehydrogenases (step 1) converts glucose 6-phosphate (G6P) to NADPH plus 6-phosphogluconolactone, which is used by 6-phosphogluconolactonases (step 2) to yield 6-phosphogluconate, the substrate of 6-phosphogluconate dehydrogenases (step 3). In this last step of the irreversible OPPP branch, another NADPH, ribulose 5-phosphate (Ru5P), and CO_2 are produced. Ru5P (or xylulose 5-phosphate) can be exchanged for orthophosphate (Pi) via pentose-phosphate transporter XPT (Eicks et al., 2002) in the inner plastid membrane. NADPH produced by the OPPP in peroxisomes may sustain critical levels of (NO) and/or Jasmonic acid (JA). For the latter, OPDA (12-oxophytodienoic acid) has to be imported from plastids. NO and JA play important roles during fertilization and seed development. For more clarity, NADPH produced in the cytosol is not shown. Abbreviations: Cyt, Cytosolic; Per, peroxisomal; and Pla, plastidial localization. Dual targeting is indicated by mixed color symbols, the *pgd2* block is high-lighted in red.

9). Therefore, the ATP-binding cassette transporter COMATOSE (CTS) in the peroxisomal membrane plays an important role for sustained JA biosynthesis (Theodoulou et al., 2005). In *cts* mutants, JA levels are reduced significantly compared with the wild type, but JA biosynthesis is not completely abolished. This indicated that, besides a fast ATP-driven transport, OPDA also may enter peroxisomes by a passive route. Inside peroxisomes, an unknown critical threshold of JA exists, and levels below this threshold can affect fertility in different ways (McConn and Browse, 1996; Footitt et al., 2007). Generally, pollen defects become obvious by a significant deviation from Mendelian genetics. In the case of single mutants affecting CTS or Kat2/Ped1 (a 3-ketoacyl-CoA thiolase involved in β-oxidation; Hayashi et al., 2002), they result from limiting JA amounts produced in peroxisomes. Hence, in heterozygous plants, mutant pollen tubes may not reach ovules before wild-type pollen tubes (Footitt et al., 2007). More severe reduction of JA synthesis, however, causes male sterility (e.g. in *cts kat2* double mutants lacking both activities).

As shown by tetrad analyses in the *qrt1-2* mutant background, *pgd2-1* pollen grains are viable and able to germinate, indicating that metabolic levels suffice to promote pollen tube outgrowth and differentiation. But certain male gametophytic defects (showing as aberrant transmission ratios) allow pollen tubes to elongate normally (Johnson-Brousseau and McCormick, 2004). Actually, there is a whole set of *hapless* (*hap*) mutants affected in critical steps of pollen tube growth and guidance (Johnson et al., 2004) whose identities still are not known, especially in class 3, subclass b (pollen tubes remaining on the septum): *hap18* and *hap22*; subclass c (pollen tubes growing normally but fail to enter the micropyle): *hap11*, *hap26*, and *hap30*; and subclass d (pollen tubes growing chaotically in the ovary): *hap24* and *hap27*. Among them may be *pgd2* and also the *abstinence by mutual consent* (*amc*) mutant (Boisson-Dernier et al., 2008), which corresponds to defective PEROXISOME BIOGENESIS FACTOR13 (Pex13p; Mano et al., 2006). Remarkably, both *amc* and *pgd2* mutants display similar transmission ratios upon reciprocal backcrossing (*AMC amc*: ♀ 45%, ♂ 34%; PGD2 *pgd2*: ♀ 46.7%, ♂ 39.5%; Tables I and II; Supplemental Fig. S10) plus lack pollen tube arrest/discharge. AMC/Pex13p is a membrane protein that forms part of the docking complex linked to transient peroxisome import pores in yeast and Arabidopsis (Meinecke et al., 2010; Woodward et al., 2014) and interacts with PTS1 receptor Pex5p in the cytosol. Pex5p was shown to be needed mainly for the import of soluble proteins with C-terminal PTS1 signal but in Arabidopsis also for those with N-terminal PTS2 signal due to interaction with the PTS2 receptor Pex7p (for review, see Lanyon-Hogg et al., 2010). Hence, in the *amc* mutant, NADPH formation inside peroxisomes should be abolished. This seems to primarily affect the OPPP branch (comprising G6PD1, PGL3, and PGD2; Meyer et al., 2011) as well as other enzymes with a PTS1 motif, like NADP-ICDH (Leterrier et al., 2012) or NADK3 (Waller et al., 2010).

Another explanation for the sterility of the *pgd2* alleles would be a substantial reduction in NO levels. Although still a matter of debate, there are two main pathways known for NO biosynthesis in plants, one depending on NADPH provision in peroxisomes (Barroso et al., 1999; Corpas et al., 2009; Corpas and Barroso, 2014b) and

the other inside plastids linked to NOA1 (formerly NOS1; Liu et al., 2010; Tewari et al., 2013). Insufficient NO levels produced in either male or female reproductive tissues can affect fertility (Prado et al., 2004; 2008). However, limiting NO synthesis in plastids seems to mainly harm the female gametophyte, usually showing as degenerated embryos in developing siliques. This resulted in about 40% less seed production by *noa1* mutants as compared with wild-type plants (Prado et al., 2008), which we did not observe for the *pgd2* mutants. Moreover, in a triple mutant with additional lack of nitrate reductase (NIA) activity in the cytosol (*nia1 nia2 noa1-2*), the accumulated NO deficiency resulted in a higher portion of aborted embryos but not in male sterility (Lozano-Juste and León, 2010a, 2010b).

NO is known to influence multiple steps during the pollen-ovary interaction, functions as a short-range guidance signal for the reorientation of pollen tubes toward ovules, and promotes further growth through the funiculus to the micropyle (for review, see Traverso et al., 2013; Domingos et al., 2015). Importantly, this involves thiol-based redox regulation, which may redirect the first two OPPP reactions from plastids to peroxisomes (Meyer et al., 2011; Hölscher et al., 2014). NO deficiency in peroxisomes can prevent the interaction/recognition of male and female gametophytes, manifesting in an absence of homozygous offspring (Prado et al., 2004; 2008). As shown recently, NO production in peroxisomes depends on Pex7p-based import of a cryptic NO synthase (Corpas and Barroso, 2014b). In light of the *amc* mutant, in which defective peroxisomal import prevents fertilization between mutant gametophytes (Boisson-Dernier et al., 2008), similar results obtained with the *pgd2* alleles clearly link OPPP reactions in peroxisomes to important steps during fertilization. Thus, sugar-derived NADPH production in peroxisomes seems to be needed to reach or maintain a critical threshold of NO and possibly also JA. These metabolic events seem to accompany the differentiation/recognition of male and female gametophytes that finally results in sperm cell delivery (Leydon et al., 2014). After successful fertilization, NO and JA are likely also important during embryo development (Supplemental Fig. S9; Goetz et al., 2012) and defense (Bosch et al., 2014), as indicated by recent studies in tomato (*Solanum lycopersicum*). Therefore, it is conceivable that our findings have important implications for other plant species and conditions in which NO and/or JA act as signaling components: in the case of peroxisomal NO during abiotic stress in roots (Corpas et al., 2009; Corpas and Barroso, 2014a) and in the case of JA during herbivory/wounding or plant-pathogen interactions. The latter are accompanied by rapid stomata closure and the inhibition of photosynthesis (Katsir et al., 2008; Campos et al., 2014; Wasternack, 2014). In tobacco leaves, this leads to callose-induced Suc retention (source-to-sink transition), which is needed for the defense of the infected tissue (Scharte et al., 2009).

CONCLUSION

We have shown that PGD2 is truly a peroxisomal and not plastidial PGD isoform. Interference with its catalytic activity prevents the interaction of male and female gametophytes in Arabidopsis and, due to conservation of the C-terminal PTS1 motif, likely also in other higher plant species. Sugar-derived NADPH provision via the OPPP in peroxisomes (Fig. 9) seems to be crucial for gametophytic interaction, especially during pollen tube guidance to ovules. Intriguingly, other reactions that may provide NADPH in peroxisomes, especially NADP-ICDH (At1g54340), for which viable mutants exist that are impaired in stomatal movements (Leterrier et al., 2015), and NADK3 (At1g78590), do not compensate, although both (according to the Arabidopsis eFP browser; Winter et al., 2007) are expressed during flower development. Possibly, their activity is either irrelevant or too low in the gametophytes to support the biosynthesis of NO and/or JA to critical levels. Whether the manipulation of OPPP steps in peroxisomes may improve plant stress tolerance and/or development via enhanced NADPH and altered metabolite levels remains to be shown by future studies.

MATERIALS AND METHODS

Bioinformatics

The Arabidopsis Information Resource home page (www.arabidopsis.org) served as a general information resource for Arabidopsis (*Arabidopsis thaliana*). Routine analyses, like mRNA expression profiles, nucleotide analyses, sequence alignments, and similarity searches, were conducted with the Arabidopsis eFP Browser (http://bbc.botany.utoronto.ca), Clustal Omega (http://www.ebi.ac.uk), the ExPASy proteomics server (http://www.expasy.ch), and the National Center for Biotechnology Information BLAST (http://blast.ncbi.nlm.nih.gov).

Arabidopsis Mutants

Information on Arabidopsis T-DNA insertion lines was retrieved from the SIGnAL database at http://signal.salk.edu (Alonso et al., 2003). Mutant lines were ordered from the Nottingham Arabidopsis Stock Centre and analyzed by PCR of genomic DNA as suggested for T-DNA insertion lines SALK_036751 (*pgd2-1*) and SALK_071687 (*pgd2-2*).

Plant Growth

Arabidopsis seeds were surface sterilized, stratified for 2 to 3 d at 4°C, and germinated on sterile one-half-strength MS agar medium (2.2 g/L MS salt mix including vitamins, pH 5.7–5.8, and 0.8% (w/v) agar; Duchefa). Plants were propagated in growth chambers under a long-day regime (16 h of light, 21°C and 8 h of darkness, 19°C) on sterile agar medium before transfer to fertilized soil mix. In the case of tobacco (*Nicotiana tabacum* var Xanthi), plants were cultivated on MS agar supplemented with 2% (w/v) Suc. After 3 to 4 weeks, shoot cuttings were transferred to fresh medium before harvesting mature leaves for protoplast isolation.

Protoplast Transfection and Microscopy

Expression of the 35S promoter-driven reporter constructs was monitored by confocal laser scanning microscopy in tobacco mesophyll protoplasts essentially as described previously (Frank et al., 2008; Meyer et al., 2011; Hölscher et al., 2014). In the case of fast protoplast preparation from soil-grown plants, leaves were harvested, surface sterilized with 70% (v/v) ethanol, and washed with sterile water before slicing them in 0.45 M mannitol as described previously.

After 1 h of incubation, mannitol was removed and 12 mL of regular enzyme solution plus 2 mL of triple-strength enzyme solution were added. Further incubation took place on a three-dimensional shaker (at 30 rpm) for 3 h at 28°C in the dark. For coexpression analyses, plasmid DNA of the test construct was premixed with 5 μg of a reporter construct prior to transfection. Protoplasts were cultivated at 21°C to 25°C in the dark and analyzed after 12 to 48 h using a confocal laser scanning microscope (Leica TCS SP2 or SP5) with excitation/emission wavelengths of 405/450 to 480 nm for CFP, 488/490 to 520 nm for GFP, 514/520 to 550 nm for YFP, and 543 or 561/590 to 620 nm for OFP (mRFP).

Reverse Transcription-PCR

Total RNA was isolated from leaves of Arabidopsis plants grown in soil using either the guanidinium-HCl procedure (Logemann et al., 1987) or the miniprep method of Sokolowsky et al. (1990). After treatment with RNase-free DNase I (Life Technologies), 5-μg aliquots were primed with 30 ng of oligo(dT) (30-mers) and reverse transcribed either by SuperScript III (Invitrogen) or AccuScript (Agilent Technologies) as recommended by the suppliers. PCR amplification from complementary DNA was conducted with 2 μL of the reverse transcription (RT) reaction and appropriate primer combinations (10 μM each) using Phusion High-Fidelity DNA Polymerase (Finnzymes).

Cloning of Fluorescent Reporter Fusions

All cloning steps followed standard protocols (Sambrook et al., 1989). Open reading frames of the candidate genes were amplified by RT-PCR from Arabidopsis leaf RNA with the primer combinations listed in Supplemental Table S1. Fluorescent reporter constructs were cloned via compatible restriction sites in plant expression vectors as described by Meyer et al. (2011) or in newly prepared pG/OFP-NX vectors (Supplemental Fig. S11). For these, pGFP2-*sdm* and pOFP2-*sdm* (with a mutated *Nco*I site in the coding region) were used as templates. First, the *Nco*I site in the 35S promoter was removed by site-directed mutagenesis (*sdm*), then the reporters were reinserted via *Xba*I and *Bam*HI after PCR amplification with primers 35S and P704 (for GFP) or P705 (for OFP). All constructs were verified by sequencing.

Site-Directed Mutagenesis

Base changes were introduced into *PGD2* by the Quick Change PCR mutagenesis protocol (Stratagene) using appropriate primer combinations (Supplemental Table S1) and Phusion High-Fidelity DNA Polymerase (Finnzymes). All base changes were confirmed by sequencing.

His-PGD2 Antiserum

The entire *PGD2* coding region was amplified by RT-PCR and subcloned in pBluescript SK for silent mutagenesis of internal *Nde*I and *Bam*HI sites. After sequence confirmation, the open reading frame was amplified with primers suited for insertion into pET16b (Novagen) via *Nde*I-*Bam*HI sites (Supplemental Table S1). Plasmid DNA of positive *Escherichia coli* XL1-blue clones was verified by sequencing and retransformed into *E. coli* BL21^{minus} (Meyer et al., 2011). Liquid cultures (YT with Clm/Tet/Amp) were induced at an optical density at 600 nm (OD_{600}) of 0.3 with isopropylthio-β-galactoside (1 mM final concentration) and harvested by centrifugation after 2 to 3 h of growth at 37°C. Cells were pelleted and frozen in liquid nitrogen (stored at −80°C) prior to lysis by sonication on ice. His-PGD2 protein was purified via Ni-NTA resin (Qiagen) under denaturing conditions using 10 mM Tris/100 mM sodium phosphate buffer (pH 8) in the presence of 0.05% (w/v) Triton X-100 and 4 M urea (without β-mercaptoethanol). After washing with 50 mM imidazole (in the above buffer), resin-bound proteins were eluted with 250 mM imidazole (in the above buffer), pooled, concentrated and desalted with a 10-kD cutoff centrifugal filter device (Amicon Ultra-4; Millipore), and used as antigen to raise a polyclonal antiserum in rabbits (Eurogentec). Recognition of recombinant PGD2 (and also recombinant PGD1 and PGD3) was confirmed by western-blot analyses.

Western-Blot Analyses

Ni-NTA samples were prepared for SDS-PAGE using loading buffer with 10 mM reduced Dithiothreitol (DTTred). Samples were boiled for 5 min and directly subjected to SDS-PAGE. After transfer to a nitrocellulose membrane, proteins were stained with Ponceau S and scanned for reference. After destaining the blot with Tris-buffered saline plus Tween 20 (TBST), the membrane was blocked with 2% (w/v) skim milk powder in TBST for at least 1 h. Incubation with PGD2 antiserum was in the same buffer (α-PGD2; 1:10,000) for 2 h at room temperature, followed by three wash steps in TBST prior to incubation with secondary antibodies (1:10,000 goat anti-rabbit horseradish peroxidase conjugate; Bio-Rad) as described previously (Frank et al., 2008; Meyer et al., 2011). After three additional wash steps, chemiluminescent signals (ECL Advance Western Blotting Detection Kit; GE Healthcare) were recorded digitally with a bioimaging system (MicroChemi DNR).

Peroxisome Purification and Activity Tests

Arabidopsis Col-0 plants grown under a short-day regime (10 h of light at 22°C/14 h of dark at 18°C) for 4 to 5 weeks were kept for 20 h in the dark before harvesting leaf blades (12 g fresh weight). Peroxisomes were purified essentially as described by Reumann et al. (2007). Aliquots were measured for the peroxisomal marker enzyme glycolate oxidase (modified acyl-CoA oxidase protocol; Gerhardt, 1983) in 175 mM Tris-HCl, pH 8.5, 13 mM *p*-hydroxybenzoic acid, 1 mM 4-aminoantipyrine, 1 mM sodium azide, 50 μM FMN, and 3.5 units of horseradish peroxidase (Serva), started with 2 mM glycolate. G6PDH activity was determined as described previously (Meyer et al., 2011), and 6PGDH activity was determined according to Bailey-Serres and Nguyen (1992) in 50 mM Tris-HCl, pH 7.5, and 0.25 mM NADP, started with 2 mM 6-phosphogluconate. GAPN activity served as a cytosolic reference (Gómez Casati et al., 2000). Glyceraldehyde-3-phosphate substrate was produced by 0.1 unit of aldolase (Sigma) in 100 mM Tris-HCL, pH 8.5, 1 mM EDTA (to inhibit NAD-dependent GAPDH), and 0.4 mM NADP, started with 0.5 mM Fru-1,6-bisP.

His-PGD2-1 Variant

Cloning of the His-PGD2-1 variant was analogous to the procedure described above for the His-PGD2 (antiserum), using RNA isolated from *pgd2-1* mutant leaves and RT-PCR with appropriate primers (listed in Supplemental Table S1). BL21^{minus} strains carrying the pET16b expression construct His-PGD2 or His-PGD2-1 were induced at 0.3 to 0.4 OD_{600} by 1 mM isopropylthio-β-galactoside and grown for 3 h at 37°C. Cells were pelleted and adjusted to 10 OD_{600} by resuspension in extraction buffer (50 mM sodium phosphate buffer, pH 7.1, 4% (v/v 87%) glycerol, 7 mM β-mercaptoethanol, 0.25 mM NADP, 1 mM Pefabloc SC [Applichem], plus protease inhibitor cocktail for use with plant extracts [Sigma]). Cells were disrupted by sonication on ice (four times 10 s) and incubated for 1 h on ice prior to pelleting debris at 4°C. Ni-NTA resin was equilibrated with binding buffer (10 mM Tris, 100 mM NaH_2PO, 150 mM NaCl adjusted to pH 8, containing 20 mM imidazole), loaded with cell lysate (diluted 1:1 with binding buffer), and washed with binding buffer (collecting 500-μL fractions). Bound proteins were eluted with 250 mM imidazole in binding buffer and checked by SDS-PAGE and activity tests: routinely, 10-μL samples were measured in 1 mL of 6PGDH assay buffer (described above). Proteins were quantified according to Bradford (1976) with acetone-washed bovine serum albumin as a reference.

Pollen Vitality and Pollen Tube Growth

After pollination of heterozygous *PGD2 pgd2-1* plants with the *qrt1-2* mutant (Preuss et al., 1994), germination of mutant and wild-type pollen tubes was scored in the F2 generation (plants forming pollen tetrads; Supplemental Fig. S7) as described by Footitt et al. (2007). For each experiment, pollen tetrads were harvested from several flowers and either stained according to Alexander (1969) with 2 mL of glacial acetic acid, as recommended for thin-walled pollen, or spread on glass coverslips with agarose-solidified germination medium. Pollen tube growth was monitored after incubation in a moist chamber as described by Bou Daher et al. (2009) and Roy et al. (2011). In vivo pollen tube staining with Aniline Blue was done essentially as described by Mori et al. (2006).

Isolation of Genomic DNA and Characterization of T-DNA Insertion Lines

Genomic DNA was isolated from 60 mg of leaf tissue (Souza-Canada, 2007). DNA fragments were amplified with Taq-DNA Polymerase (Fermentas), analyzed by gel electrophoresis, subcloned, and sequenced to identify the exact position of the T-DNA insertion. T-DNA border fragments were amplified with gene-specific LP or RP primers in combination with the appropriate T-DNA

primer (LBa1 or RBa1). The left T-DNA borders were sequenced with nested primer LBb1 (Fig. 8A).

Complementation Analyses

The entire *PGD2* sequence was amplified from genomic DNA using Phusion High-Fidelity DNA Polymerase (Finnzymes) and the indicated primer combination (listed in Supplemental Table S1). The genomic *gPGD2* fragment was inserted into *Eco*RV-opened pBluescript SK and cloned in *E. coli* XL1 blue (Stratagene). The genomic fragment was released with *Sma*I and *Sal*I and inserted into binary vector pGSC1704-HygR via *Sna*BI and *Sal*I, cloned in *E. coli* XL1 blue, and retransformed into *Agrobacterium tumefaciens* strain GV2260 as described by Scharte et al. (2009). Floral dip transformation of heterozygous plants was conducted as described by Clough and Bent (1998). Transformed seeds were selected on MS agar supplemented with hygromycin B (20 μg mL^{-1}; Roche) plus betabactyl (125 μg mL^{-1}; SmithKline Beecham) and transferred to soil at the four-leaf stage. The wild type and T-DNA alleles were scored by PCR analyses using primers binding outside or within the genomic region used for complementation (Fig. 8A; Supplemental Table S1).

Supplemental Data

The following supplemental materials are available.

Supplemental Figure S1. Amino acid alignment of PGD polypeptide sequences.

Supplemental Figure S2. Details of full-length PGD1- and PGD3-OFP fusions in tobacco protoplasts.

Supplemental Figure S3. Single channels of merged maximal projections shown in Figures 2 and 4.

Supplemental Figure S4. Localization of PGD2-reporter fusions in soil-grown Arabidopsis plants.

Supplemental Figure S5. BiFC analyses of PGD2_*C-mature* with free C-terminal ends in Arabidopsis.

Supplemental Figure S6. Ni-NTA purification of His-PGD2 and His-PGD2-1 proteins.

Supplemental Figure S7. Scheme of *pgd2-1* analyses in the *qrt1-2* background.

Supplemental Figure S8. Ni-NTA purification of His-*mature*-PGD2.

Supplemental Figure S9. Expression patterns of the three Arabidopsis *PGD* isoforms.

Supplemental Figure S10. Summary of *PGD2 pgd2* selfing and reciprocal backcrosses.

Supplemental Figure S11. Cloning scheme of the pG/OFP-NX vectors.

Supplemental Table S1. Oligonucleotide primers used in this study.

ACKNOWLEDGMENTS

We thank Wiltrud Krüger for routine laboratory support, Laura Berg for immunoblot analyses of recombinant PGD isoforms, Stephan Rips for assistance with confocal laser scanning microscopy analyses, and Leonie Steinhorst for sharing *qrt1-2* seeds plus giving advice on in vitro pollen-tube assays.

Received August 19, 2015; accepted March 2, 2016; published March 3, 2016.

LITERATURE CITED

Alexander MP (1969) Differential staining of aborted and nonaborted pollen. Stain Technol **44:** 117–122

Alonso JM, Stepanova AN, Leisse TJ, Kim CJ, Chen H, Shinn P, Stevenson DK, Zimmerman J, Barajas P, Cheuk R, et al (2003) Genome-wide insertional mutagenesis of Arabidopsis thaliana. Science **301:** 653–657

Bailey-Serres J, Nguyen MT (1992) Purification and characterization of cytosolic 6-phosphogluconate dehydrogenase isozymes from maize. Plant Physiol **100:** 1580–1583

Barroso JB, Corpas FJ, Carreras A, Sandalio LM, Valderrama R, Palma JM, Lupiáñez JA, del Río LA (1999) Localization of nitric-oxide synthase in plant peroxisomes. J Biol Chem **274:** 36729–36733

Boisson-Dernier A, Frietsch S, Kim TH, Dizon MB, Schroeder JI (2008) The peroxin loss-of-function mutation abstinence by mutual consent disrupts male-female gametophyte recognition. Curr Biol **18:** 63–68

Bosch M, Wright LP, Gershenzon J, Wasternack C, Hause B, Schaller A, Stintzi A (2014) Jasmonic acid and its precursor 12-oxophytodienoic acid control different aspects of constitutive and induced herbivore defenses in tomato. Plant Physiol **166:** 396–410

Bou Daher F, Chebli Y, Geitmann A (2009) Optimization of conditions for germination of cold-stored Arabidopsis thaliana pollen. Plant Cell Rep **28:** 347–357

Bradford MM (1976) A rapid and sensitive method for the quantitation of microgram quantities of protein utilizing the principle of protein-dye binding. Anal Biochem **72:** 248–254

Buchanan BB (1991) Regulation of CO_2 assimilation in oxygenic photosynthesis: the ferredoxin/thioredoxin system. Perspective on its discovery, present status, and future development. Arch Biochem Biophys **288:** 1–9

Bussell JD, Keech O, Fenske R, Smith SM (2013) Requirement for the plastidial oxidative pentose phosphate pathway for nitrate assimilation in Arabidopsis. Plant J **75:** 578–591

Campos ML, Kang JH, Howe GA (2014) Jasmonate-triggered plant immunity. J Chem Ecol **40:** 657–675

Chai MF, Wei PC, Chen QJ, An R, Chen J, Yang S, Wang XC (2006) NADK3, a novel cytoplasmic source of NADPH, is required under conditions of oxidative stress and modulates abscisic acid responses in Arabidopsis. Plant J **47:** 665–674

Clough SJ, Bent AF (1998) Floral dip: a simplified method for Agrobacterium-mediated transformation of Arabidopsis thaliana. Plant J **16:** 735–743

Copenhaver GP, Browne WE, Preuss D (1998) Assaying genome-wide recombination and centromere functions with Arabidopsis tetrads. Proc Natl Acad Sci USA **95:** 247–252

Corpas FJ, Barroso JB (2014a) Peroxynitrite (ONOO-) is endogenously produced in Arabidopsis peroxisomes and is overproduced under cadmium stress. Ann Bot (Lond) **113:** 87–96

Corpas FJ, Barroso JB (2014b) Peroxisomal plant nitric oxide synthase (NOS) protein is imported by peroxisomal targeting signal type 2 (PTS2) in a process that depends on the cytosolic receptor PEX7 and calmodulin. FEBS Lett **588:** 2049–2054

Corpas FJ, Barroso JB, Sandalio LM, Distefano S, Palma JM, Lupiáñez JA, Del Río LA (1998) A dehydrogenase-mediated recycling system of NADPH in plant peroxisomes. Biochem J **330:** 777–784

Corpas FJ, Hayashi M, Mano S, Nishimura M, Barroso JB (2009) Peroxisomes are required for in vivo nitric oxide accumulation in the cytosol following salinity stress of Arabidopsis plants. Plant Physiol **151:** 2083–2094

Desfeux C, Clough SJ, Bent AF (2000) Female reproductive tissues are the primary target of Agrobacterium-mediated transformation by the Arabidopsis floral-dip method. Plant Physiol **123:** 895–904

Dietz KJ (2015) Efficient high light acclimation involves rapid processes at multiple mechanistic levels. J Exp Bot **66:** 2401–2414

Domingos P, Prado AM, Wong A, Gehring C, Feijo JA (2015) Nitric oxide: a multitasked signaling gas in plants. Mol Plant **8:** 506–520

Eicks M, Maurino V, Knappe S, Flügge UI, Fischer K (2002) The plastidic pentose phosphate translocator represents a link between the cytosolic and the plastidic pentose phosphate pathways in plants. Plant Physiol **128:** 512–522

Eubel H, Meyer EH, Taylor NL, Bussell JD, O'Toole N, Heazlewood JL, Castleden I, Small ID, Smith SM, Millar AH (2008) Novel proteins, putative membrane transporters, and an integrated metabolic network are revealed by quantitative proteomic analysis of Arabidopsis cell culture peroxisomes. Plant Physiol **148:** 1809–1829

Footitt S, Dietrich D, Fait A, Fernie AR, Holdsworth MJ, Baker A, Theodoulou FL (2007) The COMATOSE ATP-binding cassette transporter is required for full fertility in Arabidopsis. Plant Physiol **144:** 1467–1480

Francis KE, Lam SY, Copenhaver GP (2006) Separation of Arabidopsis pollen tetrads is regulated by QUARTET1, a pectin methylesterase gene. Plant Physiol **142:** 1004–1013

Frank J, Kaulfürst-Soboll H, Rips S, Koiwa H, von Schaewen A (2008) Comparative analyses of Arabidopsis *complex glycan1* mutants and genetic interaction with *staurosporin and temperature sensitive3a*. Plant Physiol **148:** 1354–1367

Gerhardt B (1983) Localization of β-oxidation enzymes in peroxisomes isolated from nonfatty plant tissues. Planta **159:** 238–246

Goepfert S, Poirier Y (2007) Beta-oxidation in fatty acid degradation and beyond. Curr Opin Plant Biol **10:** 245–251

Goetz S, Hellwege A, Stenzel I, Kutter C, Hauptmann V, Forner S, McCaig B, Hause G, Miersch O, Wasternack C, et al (2012) Role of cis-12-oxo-phytodienoic acid in tomato embryo development. Plant Physiol **158:** 1715–1727

Gómez Casati DF, Sesma JI, Iglesias AA (2000) Structural and kinetic characterization of NADP-dependent, non-phosphorylating glyceraldehyde-3-phosphate dehydrogenase from celery leaves. Plant Sci **154:** 107–115

Graham IA, Eastmond PJ (2002) Pathways of straight and branched chain fatty acid catabolism in higher plants. Prog Lipid Res **41:** 156–181

Hayashi M, Nito K, Takei-Hoshi R, Yagi M, Kondo M, Suenaga A, Yamaya T, Nishimura M (2002) Ped3p is a peroxisomal ATP-binding cassette transporter that might supply substrates for fatty acid beta-oxidation. Plant Cell Physiol **43:** 1–11

Hölscher C, Meyer T, von Schaewen A (2014) Dual-targeting of Arabidopsis 6-phosphogluconolactonase 3 (PGL3) to chloroplasts and peroxisomes involves interaction with Trx m2 in the cytosol. Mol Plant **7:** 252–255

Hu J, Baker A, Bartel B, Linka N, Mullen RT, Reumann S, Zolman BK (2012) Plant peroxisomes: biogenesis and function. Plant Cell **24:** 2279–2303

Johnson MA, von Besser K, Zhou Q, Smith E, Aux G, Patton D, Levin JZ, Preuss D (2004) Arabidopsis hapless mutations define essential gametophytic functions. Genetics **168:** 971–982

Johnson-Brousseau SA, McCormick S (2004) A compendium of methods useful for characterizing Arabidopsis pollen mutants and gametophytically-expressed genes. Plant J **39:** 761–775

Katsir L, Chung HS, Koo AJK, Howe GA (2008) Jasmonate signaling: a conserved mechanism of hormone sensing. Curr Opin Plant Biol **11:** 428–435

Krepinsky K, Plaumann M, Martin W, Schnarrenberger C (2001) Purification and cloning of chloroplast 6-phosphogluconate dehydrogenase from spinach: cyanobacterial genes for chloroplast and cytosolic isoenzymes encoded in eukaryotic chromosomes. Eur J Biochem **268:** 2678–2686

Kruger NJ, von Schaewen A (2003) The oxidative pentose phosphate pathway: structure and organisation. Curr Opin Plant Biol **6:** 236–246

Lanyon-Hogg T, Warriner SL, Baker A (2010) Getting a camel through the eye of a needle: the import of folded proteins by peroxisomes. Biol Cell **102:** 245–263

Leterrier M, Barroso JB, Valderrama R, Begara-Morales JC, Sánchez-Calvo B, Chaki M, Luque F, Viñegla B, Palma JM, Corpas FJ (2015) Peroxisomal NADP-isocitrate dehydrogenase is required for Arabidopsis stomatal movement. Protoplasma **253:** 403–415

Leterrier M, Barroso JB, Valderrama R, Palma JM, Corpas FJ (2012) NADP-dependent isocitrate dehydrogenase from Arabidopsis roots contributes in the mechanism of defence against the nitro-oxidative stress induced by salinity. ScientificWorldJournal **2012:** 694740

Leydon AR, Chaibang A, Johnson MA (2014) Interactions between pollen tube and pistil control pollen tube identity and sperm release in the Arabidopsis female gametophyte. Biochem Soc Trans **42:** 340–345

Liu Y, Jiang H, Zhao Z, An L (2010) Nitric oxide synthase like activity-dependent nitric oxide production protects against chilling-induced oxidative damage in Chorispora bungeana suspension cultured cells. Plant Physiol Biochem **48:** 936–944

Logemann J, Schell J, Willmitzer L (1987) Improved method for the isolation of RNA from plant tissues. Anal Biochem **163:** 16–20

Lozano-Juste J, León J (2010a) Enhanced abscisic acid-mediated responses in *nia1nia2noa1-2* triple mutant impaired in NIA/NR- and AtNOA1-dependent nitric oxide biosynthesis in Arabidopsis. Plant Physiol **152:** 891–903

Lozano-Juste J, León J (2010b) Nitric oxide modulates sensitivity to ABA. Plant Signal Behav **5:** 314–316

Mano S, Nakamori C, Nito K, Kondo M, Nishimura M (2006) The Arabidopsis pex12 and pex13 mutants are defective in both PTS1- and PTS2-dependent protein transport to peroxisomes. Plant J **47:** 604–618

McConn M, Browse J (1996) The critical requirement for linolenic acid is pollen development, not photosynthesis, in an *Arabidopsis* mutant. Plant Cell **8:** 403–416

Meinecke M, Cizmowski C, Schliebs W, Krüger V, Beck S, Wagner R, Erdmann R (2010) The peroxisomal importomer constitutes a large and highly dynamic pore. Nat Cell Biol **12:** 273–277

Meinke D, Muralla R, Sweeney C, Dickerman A (2008) Identifying essential genes in Arabidopsis thaliana. Trends Plant Sci **13:** 483–491

Meyer T, Hölscher C, Schwöppe C, von Schaewen A (2011) Alternative targeting of Arabidopsis plastidic glucose-6-phosphate dehydrogenase G6PD1 involves cysteine-dependent interaction with G6PD4 in the cytosol. Plant J **66:** 745–758

Mori T, Kuroiwa H, Higashiyama T, Kuroiwa T (2006) GENERATIVE CELL SPECIFIC 1 is essential for angiosperm fertilization. Nat Cell Biol **8:** 64–71

Niewiadomski P, Knappe S, Geimer S, Fischer K, Schulz B, Unte US, Rosso MG, Ache P, Flügge UI, Schneider A (2005) The *Arabidopsis* plastidic glucose 6-phosphate/phosphate translocator GPT1 is essential for pollen maturation and embryo sac development. Plant Cell **17:** 760–775

Noctor G, Mhamdi A, Chaouch S, Han Y, Neukermans J, Marquez-Garcia B, Queval G, Foyer CH (2012) Glutathione in plants: an integrated overview. Plant Cell Environ **35:** 454–484

Phillips C, Dohnalek J, Gover S, Barrett MP, Adams MJ (1998) A 2.8 A resolution structure of 6-phosphogluconate dehydrogenase from the protozoan parasite Trypanosoma brucei: comparison with the sheep enzyme accounts for differences in activity with coenzyme and substrate analogues. J Mol Biol **282:** 667–681

Prado AM, Colaço R, Moreno N, Silva AC, Feijó JA (2008) Targeting of pollen tubes to ovules is dependent on nitric oxide (NO) signaling. Mol Plant **1:** 703–714

Prado AM, Porterfield DM, Feijó JA (2004) Nitric oxide is involved in growth regulation and re-orientation of pollen tubes. Development **131:** 2707–2714

Preuss D, Rhee SY, Davis RW (1994) Tetrad analysis possible in Arabidopsis with mutation of the QUARTET (QRT) genes. Science **264:** 1458–1460

Quan S, Yang P, Cassin-Ross G, Kaur N, Switzenberg R, Aung K, Li J, Hu J (2013) Proteome analysis of peroxisomes from etiolated Arabidopsis seedlings identifies a peroxisomal protease involved in β-oxidation and development. Plant Physiol **163:** 1518–1538

Reumann S (2004) Specification of the peroxisome targeting signals type 1 and type 2 of plant peroxisomes by bioinformatics analyses. Plant Physiol **135:** 783–800

Reumann S, Babujee L, Ma C, Wienkoop S, Siemsen T, Antonicelli GE, Rasche N, Lüder F, Weckwerth W, Jahn O (2007) Proteome analysis of *Arabidopsis* leaf peroxisomes reveals novel targeting peptides, metabolic pathways, and defense mechanisms. Plant Cell **19:** 3170–3193

Reumann S, Ma C, Lemke S, Babujee L (2004) AraPerox: a database of putative Arabidopsis proteins from plant peroxisomes. Plant Physiol **136:** 2587–2608

Roy B, Copenhaver GP, von Arnim AG (2011) Fluorescence-tagged transgenic lines reveal genetic defects in pollen growth: application to the eIF3 complex. PLoS ONE **6:** e17640

Sambrook J, Fritsch EF, Maniatis T (1989) Molecular Cloning: A Laboratory Manual, Ed 2. Cold Spring Harbor Laboratory Press, Cold Spring Harbor, NY

Schaller A, Stintzi A (2009) Enzymes in jasmonate biosynthesis: structure, function, regulation. Phytochemistry **70:** 1532–1538

Scharte J, Schön H, Tjaden Z, Weis E, von Schaewen A (2009) Isoenzyme replacement of glucose-6-phosphate dehydrogenase in the cytosol improves stress tolerance in plants. Proc Natl Acad Sci USA **106:** 8061–8066

Scheibe R (1991) Redox-modulation of chloroplast enzymes: a common principle for individual control. Plant Physiol **96:** 1–3

Schmid M, Davison TS, Henz SR, Pape UJ, Demar M, Vingron M, Schölkopf B, Weigel D, Lohmann JU (2005) A gene expression map of Arabidopsis thaliana development. Nat Genet **37:** 501–506

Schnarrenberger C, Flechner A, Martin W (1995) Enzymatic evidence for a complete oxidative pentose phosphate pathway in chloroplasts and an incomplete pathway in the cytosol of spinach leaves. Plant Physiol **108:** 609–614

Selinski J, Scheibe R (2014) Pollen tube growth: where does the energy come from? Plant Signal Behav **9:** e977200

Sokolowsky V, Kaldenhoff R, Ricci M, Russo VEA (1990) Fast and reliable mini-prep RNA extraction from Neurospora crassa. Fungal Genet Newsl **36:** 41–43

Souza-Canada ED (2007) Homemade protocol instead of DNA-extraction kit. Lab Times **3:** 51

Stintzi A, Browse J (2000) The Arabidopsis male-sterile mutant, opr3, lacks the 12-oxophytodienoic acid reductase required for jasmonate synthesis. Proc Natl Acad Sci USA **97:** 10625–10630

Tewari RK, Prommer J, Watanabe M (2013) Endogenous nitric oxide generation in protoplast chloroplasts. Plant Cell Rep **32:** 31–44

Theodoulou FL, Job K, Slocombe SP, Footitt S, Holdsworth M, Baker A, Larson TR, Graham IA (2005) Jasmonic acid levels are reduced in COMATOSE ATP-binding cassette transporter mutants: implications for transport of jasmonate precursors into peroxisomes. Plant Physiol **137:** 835–840

Traverso JA, Pulido A, Rodríguez-García MI, Alché JD (2013) Thiol-based redox regulation in sexual plant reproduction: new insights and perspectives. Front Plant Sci **4:** 465

Waller JC, Dhanoa PK, Schumann U, Mullen RT, Snedden WA (2010) Subcellular and tissue localization of NAD kinases from Arabidopsis: compartmentalization of de novo NADP biosynthesis. Planta **231:** 305–317

Walter M, Chaban C, Schütze K, Batistic O, Weckermann K, Näke C, Blazevic D, Grefen C, Schumacher K, Oecking C, et al (2004) Visualization of protein interactions in living plant cells using bimolecular fluorescence complementation. Plant J **40:** 428–438

Wasternack C (2014) Action of jasmonates in plant stress responses and development: applied aspects. Biotechnol Adv **32:** 31–39

Winter D, Vinegar B, Nahal H, Ammar R, Wilson GV, Provart NJ (2007) An "Electronic Fluorescent Pictograph" browser for exploring and analyzing large-scale biological data sets. PLoS ONE **2:** e718

Woodward AW, Fleming WA, Burkhart SE, Ratzel SE, Bjornson M, Bartel B (2014) A viable Arabidopsis pex13 missense allele confers severe peroxisomal defects and decreases PEX5 association with peroxisomes. Plant Mol Biol **86:** 201–214

Xiong Y, DeFraia C, Williams D, Zhang X, Mou Z (2009) Characterization of Arabidopsis 6-phosphogluconolactonase T-DNA insertion mutants reveals an essential role for the oxidative section of the plastidic pentose phosphate pathway in plant growth and development. Plant Cell Physiol **50:** 1277–1291